Rapid Communications

Coping with spurious radiation in binary black hole simulations

Kenny Higginbotham, Bhavesh Khamesra, James P. McInerney, Karan Jani, Deirdre M. Shoemaker, and Pablo Laguna
Center for Relativistic Astrophysics, School of Physics, Georgia Institute of Technology, Atlanta, Georgia 30332

(Received 2 July 2019; published 4 October 2019)

Spurious radiation in the initial data for binary black hole numerical simulations has been an issue of concern. The radiation affects the masses and spins of the black holes, modifying their orbital dynamics and thus potentially compromising the accuracy of templates used in gravitational wave analysis. Our study finds that spurious radiation effects are localized to the vicinity of the black holes. Using insights from single black hole simulations, we obtain fitting formulas to estimate the changes from spurious radiation on the mass and spin magnitude of the black holes in binary systems. We demonstrate how these fitting formulas could be used to adjust the initial masses and spin magnitudes of the black holes, so the resulting binary has the desired parameters after the spurious radiation has left the computational domain. A comparison of waveforms from raw simulations with those from simulations that have been adjusted for spurious radiation demonstrate that spurious radiation could have an appreciable effect on the templates for LIGO sources with SNRs above 30.

DOI: 10.1103/PhysRevD.100.081501

I. INTRODUCTION

This paper presents a method to deal with the *spurious* radiation in puncture-type initial data for binary black hole (BBH) simulations.

When general relativity is viewed as an initial-value problem, the initial data consist of the spatial metric γ_{ij} and the extrinsic curvature K_{ij} of the initial hypersurface in the space-time foliation. In the pair $\{\gamma_{ij}, K_{ij}\}$, not everything is freely specifiable. Four *pieces* are fixed by the Hamiltonian and momentum constraints. The York-Lichnerowicz approach [1,2] provides a path to identify those pieces via conformal transformations and transverse-traceless decompositions. With this approach, after assuming conformal flatness ($\gamma_{ij} = \Phi^4\eta_{ij}$) and vanishing trace of the extrinsic curvature ($K^i_i = 0$), the Hamiltonian constraint for vacuum space-times reads $\tilde{\Delta}\Phi + \Phi^{-7}\tilde{A}_{ij}\tilde{A}^{ij}/8 = 0$. Here, tildes denote tensors and operators in conformal space, and $\tilde{A}_{ij}$ is the conformal trace-free extrinsic curvature satisfying the momentum constraint $\tilde{\nabla}_i\tilde{A}^{ij} = 0$.

To construct BBH puncture-type initial data, one uses the Bowen-York [3] solutions to $\tilde{\nabla}_i\tilde{A}^{ij} = 0$. They are $\tilde{A}^{ij} = 3[P^i l^j + P^j l^i - (\eta^{ij} - l^i l^j)(P^k l_k)]/(2r^2)$ and $\tilde{A}^{ij} = 6l^{(i}\epsilon^{j)kl}S_k l_l/r^3$, with $l^i = x^i/r$ and ϵ^{ijk} the Levi-Civita symbol. Here, P^i and S^i are the linear and angular momentum of the point source, respectively. Given these solutions, the Hamiltonian constraint is solved using the *puncture* approach [4], in which $\Phi = 1 + m_1/|r - r_1| + m_2/|r - r_2| + u$, with $r_{1,2}$ the locations of the black holes (BHs) and u a regular function. The parameters $m_{1,2}$ are the *bare* or puncture masses.

Puncture-type BBH initial data are then fully characterized by the parameters $m_{1,2}$, $r_{1,2}$, $P^i_{1,2}$ and $S^i_{1,2}$. The most common approach to fix these parameters is with the assistance of post-Newtonian (PN) approximations. PN equations of motion are used to evolve the BBH of interest from large separations until the separation at which the numerical relativity (NR) evolution will start. The parameters at the end of the PN evolution are used as input parameters to solve the Hamiltonian constraint. There is a subtlety here. The bare puncture masses $m_{1,2}$ are not the masses of the BHs. As a first guess for these parameters, one uses the PN BH masses, but iterations are needed to adjust the puncture bare masses until the masses of the BHs match the desired PN masses.

There is an issue with the puncture BBH initial data as just described. For sufficiently large binary separations, one would expect the space-time in the neighborhood of each BH to be close to a boosted Kerr solution, or boosted Schwarzschild solution if the BH is not spinning. This is not the case for the puncture data with Bowen-York extrinsic curvatures, not even for a single BH. The reasons for this are the conformal flatness assumption and the Bowen-York extrinsic curvatures. The space-time of a boosted or a Kerr BH is not conformally flat. Also, the Bowen-York extrinsic curvatures are not the extrinsic curvatures for a boosted or Kerr BH. As a consequence, the puncture Bowen-York initial data contain *spurious* radiation.

Spurious radiation manifests itself as a burst. Figure 1 depicts an example in terms of the Weyl scalar Ψ_4. There is an ongoing debate in the NR community about the extent to which the spurious radiation introduces appreciable

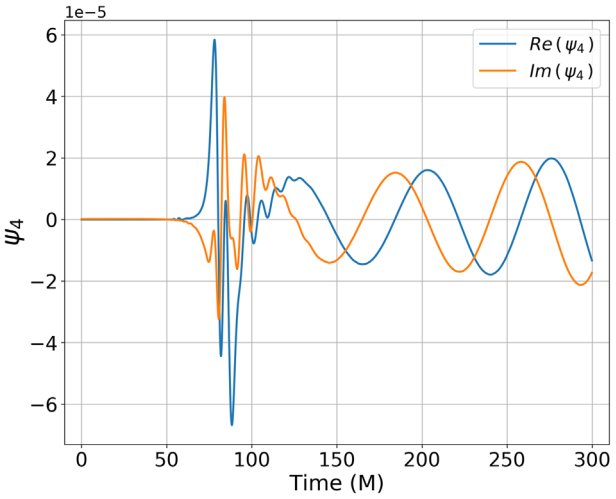

FIG. 1. Mode (2,2) of the Weyl scalar Ψ_4 extracted at a radius $75\,M$ for the waveform GT0860, an equal mass, precessing BBH system. The spurious radiation is evident at the beginning.

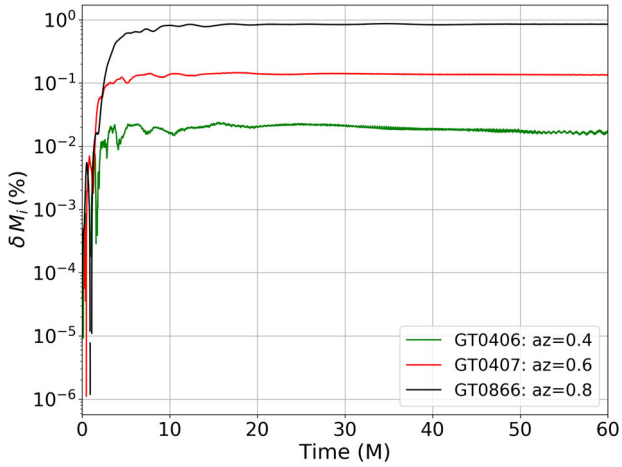

FIG. 2. The percent change in initial irreducible mass of the BHs for three simulations in the Georgia Tech catalog.

changes to the binary, specifically changes to the spins and masses of the BHs, and thus to the orbital dynamics of the binary [5–13]. Some of the studies attempt to tame the spurious radiation by moving away from conformal flatness [6,7], others introduce explicitly PN corrections [9]. Our view here is to obtain first a detailed characterization of the effects from spurious radiation on the holes and then introduce adjustments in the input parameters of the binary that anticipates the changes produced by the spurious radiation. The expectation is that, after the spurious radiation dissipates away, one is left with the BBH system one originally intends to have.

II. WAVEFORM ANALYSIS

Our work is based on the Georgia Tech catalog of BBH simulations [14]. The first step was to monitor in our simulations the behavior of the masses and spins of the BHs in a window between the initial time of the simulation and the end of the burst of spurious radiation. Figure 2 shows the percent change δM_i in the initial irreducible mass of the BHs in time for three binary simulations from the catalog: GT0406, GT0407 and GT0866. The irreducible mass M_i is computed from the area A of BH horizon: $M_i = \sqrt{A/4\pi}$. It is evident in Fig. 2 the increase in the masses of the BHs during the first $20\,M$ of the simulation. This trend was observed in all the simulations for which we tracked the masses of the holes. Similar jumps were also observed in the spins.

A. Learning from single black hole simulations

Next we investigated whether the jumps in mass and spin were due to *local* effects in the neighborhood of the BHs or if they involved correlations between the holes in the binaries. To answer this, we looked at the effects of spurious radiation on a single BH. We carried out simulations expanding the dimensionless spin parameter $a = S/M_h^2$ in the range $0 \le a \le 0.8$ and the speed $v = P/M_h$ in the range $0 \le v \le 0.3$, with S the angular momentum, P the

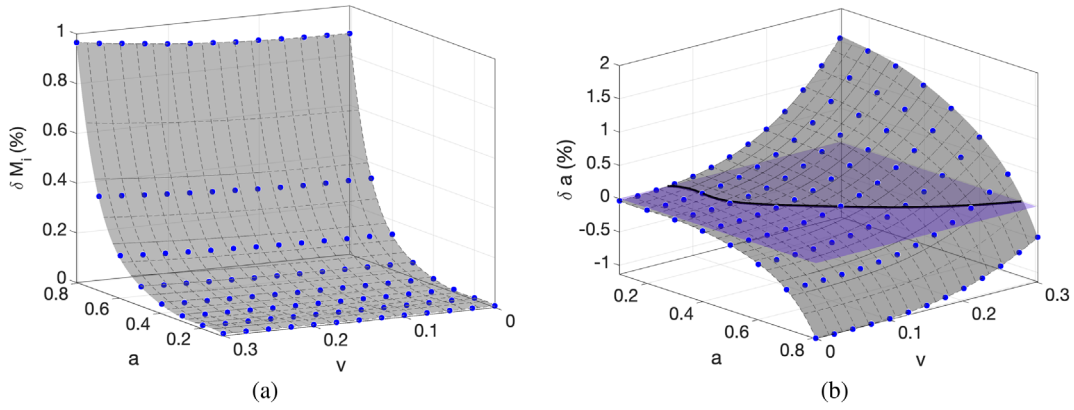

FIG. 3. Percent change in irreducible mass (a) and spin (b) in the single BH simulations (blue dots). Two-parameter fits to the data by Eq. (1) are shown as gray surfaces.

TABLE I. Fitting coefficients for δM_i and δa in Eq. (1).

c_{ij}	δM_i	δa	c_{ij}	δM_i	δa
c_{00}	−0.09935	0.1294	c_{40}	−65.83	79.59
c_{10}	2.148	−3.169	c_{31}	−4.27	13.47
c_{01}	0.05612	−0.0977	c_{22}	−1.565	−5.56
c_{20}	−14.92	21.01	c_{13}	3.918	−13.17
c_{11}	−0.4674	1.118	c_{04}	−21.74	288.9
c_{02}	−0.6845	7.696	c_{50}	36.64	−40.72
c_{30}	46.3	−61.24	c_{41}	2.524	−7.763
c_{21}	2.386	−7.675	c_{32}	2.931	2.056
c_{12}	−0.2141	2.781	c_{23}	−0.7278	−35.24
c_{03}	5.791	−15.01	c_{14}	−5.623	12.7
			c_{05}	29.78	−413.8

linear momentum, and M_h the mass of the BH, where $M_h^2 = M_i^2 + S^2/(2M_i)^2$. The spin of the BH was aligned with the z-direction and the momentum with the y-direction. To a good approximation, these configurations cover the initial setups of BHs in the nonprecessing simulations.

Not surprisingly, the single BH simulations also showed increases in mass and spin. Furthermore, those increases took place, as with the BBH simulations, during the first $20M$ of the simulation time. This suggests that the effects of spurious radiation are localized near the hole and do not depend on the presence of the other hole.

Figure 3 shows with points the percentage change in the BH irreducible mass δM_i and δa for all the single BH simulations as a function of the dimensionless spin a and speed v. The gray surfaces in Fig. 3 are fits to

$$\begin{aligned} F = {} & c_{00} + c_{10}a + c_{20}a^2 + c_{30}a^3 + c_{40}a^4 + c_{50}a^5 \\ & + c_{01}v + c_{02}v^2 + c_{03}v^3 + c_{04}v^4 + c_{05}v^5 \\ & + c_{11}av + c_{12}av^2 + c_{13}av^3 + c_{14}av^4 \\ & + c_{21}a^2v + c_{31}a^3v + c_{41}a^4v \\ & + c_{22}a^2v^2 + c_{23}a^2v^3 + c_{32}a^3v^2. \end{aligned} \tag{1}$$

The coefficients for the fit to δM_i and δa are given in Table I.

Interestingly, from Fig. 3(a), the effect of spurious radiation on the mass correlates stronger with the initial spin than with the speed of the puncture. This is not the case with the effect on the spin of the BH. As it can be seen from

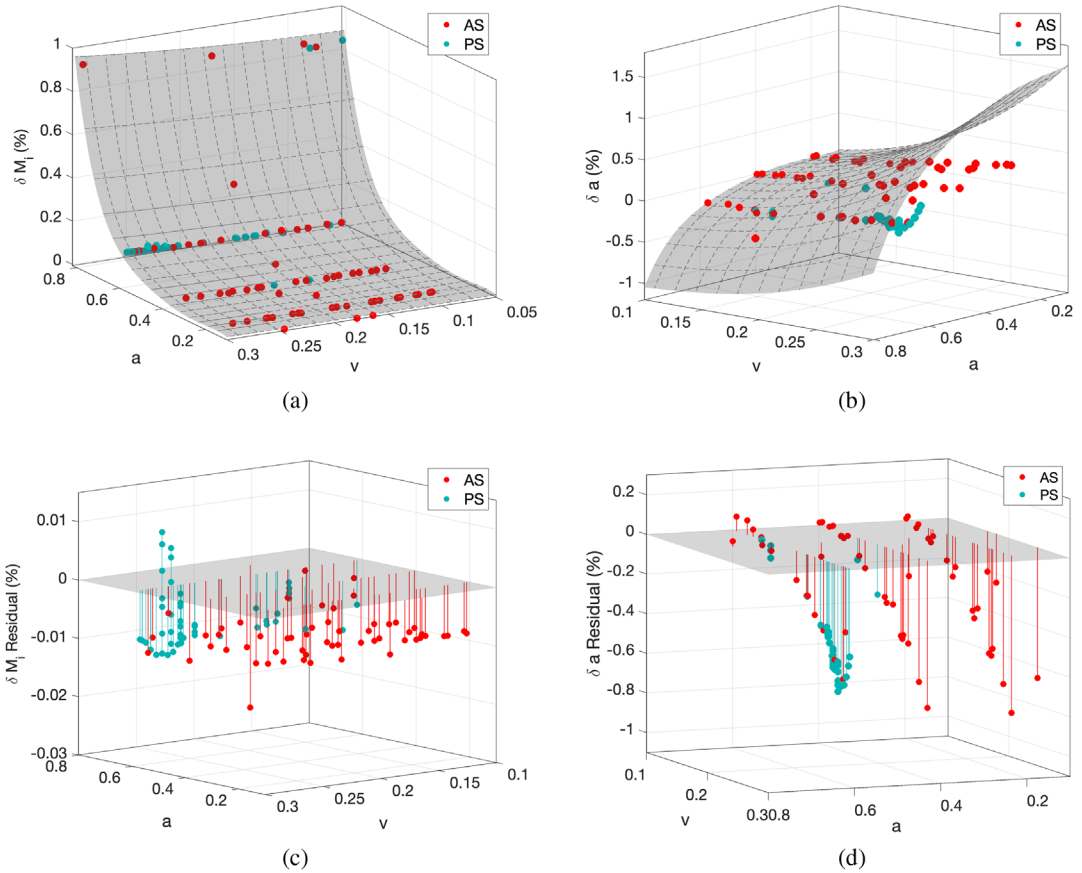

FIG. 4. A comparison of the percent changes (a) δM_i and (b) δa in BBH simulations (red for aligned spins and green for precessing binaries) with the single BH fit (gray surface). Residuals ≔ (data fit) between the single BH fit and the BBH data are shown in (c) and (d).

Fig. 3(b), the spurious radiation reduces the spin for larger initial spin and increases the spin for larger speeds. As a consequence, there is a family of cases for which the effects cancel out. These are the cases when the surface in Fig. 3(b) intersects the $\delta a = 0$ plane, and they are denoted with the black line. Another important finding was that the spurious radiation only affected the magnitude of the spin but not its direction.

B. Connecting with binary black hole simulations

The next step was to investigate whether these changes are the same as those observed in each of the holes in BBH simulations. We looked at 107 binary simulations in our catalog: 67 precessing binaries, and 40 aligned spin, nonprecessing binaries. Figures 4(a) and 4(b) show with points δM_i and δa for the BHs in the BBHs (red for aligned spins and green points for precessing binaries). Gray surfaces denote the single BH fit. Figures 4(c) and 4(d) show the corresponding residuals. The residuals in the masses are $O(10^{-2})\%$, and for $v \leq 0.24$ the spin residuals are $O(10^{-1})\%$. On the other hand, for $v \gtrsim 0.24$ the spin residuals are $O(1)\%$ and all negative. Since the residuals are data fit, this implies that the single BH fit overestimates the effect of spurious radiation for $v \gtrsim 0.24$. For reference, BHs with $v \approx 0.24$ involve binary systems with initial separations of $\approx 10M$ and gravitational wave frequency $\omega M \approx 0.048$. The levels of residuals for δM_i and for δa if $v \lesssim 0.24$ give us confidence that the fitting formula derived from single BH simulations provides good estimates applicable to binary simulations.

C. When to worry about spurious radiation

Finally, we present a couple of examples of how the single BH spurious radiation fits can be used in BBH simulations. Assuming that one wants to simulate a binary with BHs having irreducible masses $M_i^{1,2}$, spins $a^{1,2}$ and speeds $v^{1,2}$, the task is to find irreducible masses $\bar{M}_i^{1,2}$ and spins $\bar{a}^{1,2}$ to use in the initial data such that the spurious radiation modifies these values and yields the desired values $M_i^{1,2}$ and $a^{1,2}$. The adjusted values $\bar{M}_i^{1,2}$ and $\bar{a}^{1,2}$ can be found by solving $M_i^{1,2} = [1 + \delta\bar{M}_i^{1,2}(\bar{a}^{1,2}, v^{1,2})]\bar{M}_i^{1,2}$ and $a^{1,2} = [1 + \delta\bar{a}^{1,2}(\bar{a}^{1,2}, v^{1,2})]\bar{a}^{1,2}$, where the spurious radiation changes are given as fractional changes not percentages. As mentioned before, for BHs moving with speeds $\gtrsim 0.24$, the formulas overestimate the correction on the spin magnitude. For those cases, we estimate that only a 10% correction should be applied.

Figure 5 depicts the (2,2) mode of Weyl scalar Ψ_4 for two pairs of simulations. All four simulations consist of equal mass, aligned spin binaries. The top panel shows the cases with $a \approx 0.6$ and the bottom for $a \approx 0.8$. In blue is the waveform from the *raw* simulation and in orange the waveform in which the masses and spins have been adjusted according to the single BH fitting formulas. The mass of the BH, its irreducible mass and spin magnitude at the beginning of the simulation and after the spurious radiation has dissipated are given in Table II. Notice that with the spurious adjustment $M_i/M(t > t_{\rm sp};{\rm adj}) \approx M_i/M(t=0;{\rm raw})$ and $a(t > t_{\rm sp};{\rm adj}) \approx a(t = 0;{\rm raw})$, as needed.

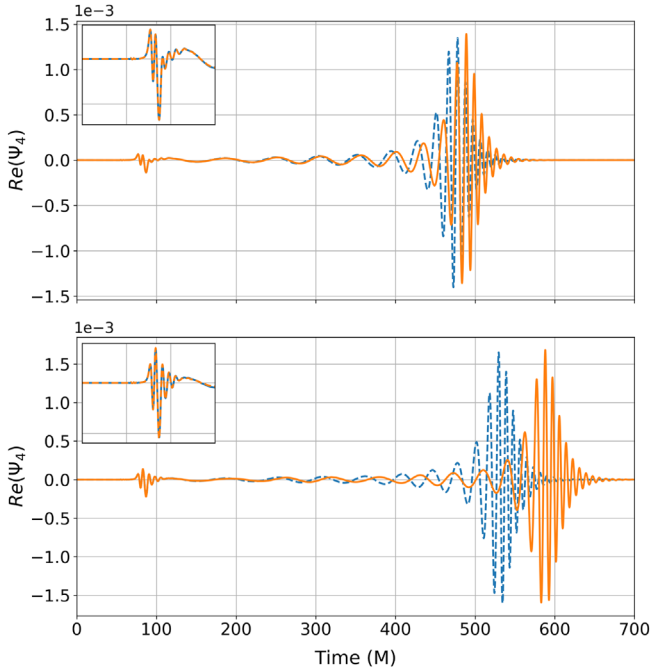

FIG. 5. Mode (2,2) of Ψ_4 for two equal mass, aligned spin binaries. Top panel shows $a \approx 0.6$ and the bottom $a \approx 0.8$. Blue waveform is from the *raw* simulation and orange waveform from the adjusted simulation. Insets focus on the spurious radiation.

The mismatches ϵ between the waveform from *raw* and adjusted simulations in Advanced LIGO are shown in Fig. 6. For $a \approx 0.8$, $\epsilon \sim 10^{-3}$ on average, while for $a \approx 0.6$, $\epsilon \sim 10^{-5}$. To avoid astrophysical inference with a bias, one needs $\epsilon\rho^2 \lesssim 1$ [15]. This implies that waveforms of sources with highly spinning BH measured with S/N of $\rho \gtrsim 30$ will exhibit inference biases if they are not corrected for the spurious radiation. For future detectors such as the Einstein Telescope and LISA, even

TABLE II. BH mass and spin at the beginning and after the spurious radiation has dissipated.

	$t = 0$			$t > t_{\rm sp}$		
Type	M_h/M	M_i/M	a	M_h/M	M_i/M	a
Raw	0.4994	0.4736	0.6013	0.5004	0.4744	0.6032
Adj	0.4985	0.4729	0.6000	0.4994	0.4736	0.6018
Raw	0.4972	0.4430	0.8090	0.5001	0.4471	0.8013
Adj	0.4939	0.4387	0.8161	0.4971	0.4431	0.8079

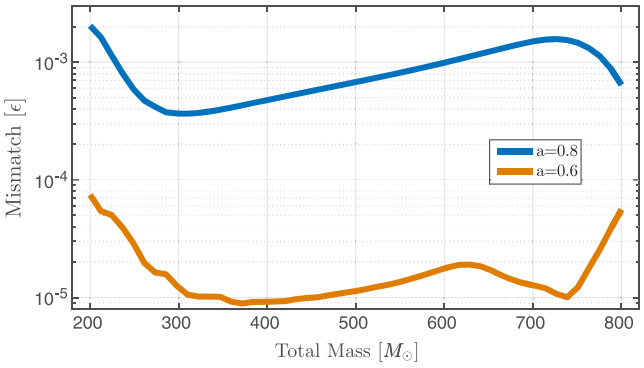

FIG. 6. Mismatches as a function of total mass of the binary for waveforms between *raw* and adjusted waveforms. Blue refers $a \approx 0.6$ and yellow to $a \approx 0.8$. Mismatches computed for Advanced LIGO design noise and masses in the detector frame.

low spin sources with $\rho \gtrsim 10^2$ would require spurious radiation correction.

III. CONCLUSION

Using simulations of single punctures with different spins and linear momentum, we investigated the effect of spurious radiation on the mass and spin of the BH. We found that spurious radiation does not affect the direction of the spin. With these results, we obtained fitting functions that can be used to predict changes in the masses and spin magnitudes of BHs in binary systems. We tested the effectiveness of the fitting functions and showed that for binary systems with highly spinning BHs, inference biases would be introduced by waveforms that not are corrected for spurious radiation in sources with SNRs $\gtrsim$30.

ACKNOWLEDGMENTS

Work supported by NSF Grants No. 1806580, No. 1809572, No. 1550461, and Extreme Science and Engineering Discovery Environment (XSEDE) Allocation No. TG-PHY120016.

[1] T. W. Baumgarte and S. L. Shapiro, *Numerical Relativity: Solving Einstein's Equations on the Computer* (Cambridge University Press, Cambridge, England, 2010).
[2] *Sources of Gravitational Radiation*, edited by L. L. Smarr (Cambridge university press, 1979).
[3] J. M. Bowen and J. W. York, Jr., Phys. Rev. D **21**, 2047 (1980).
[4] S. Brandt and B. Bruegmann, Phys. Rev. Lett. **78**, 3606 (1997).
[5] M. Hannam, S. Husa, B. Brügmann, J. A. González, and U. Sperhake, Classical Quantum Gravity **24**, S15 (2007).
[6] G. Lovelace, Classical Quantum Gravity **26**, 114002 (2009).
[7] N. K. Johnson-McDaniel, N. Yunes, W. Tichy, and B. J. Owen, Phys. Rev. D **80**, 124039 (2009).
[8] T. Chu, H. P. Pfeiffer, and M. A. Scheel, Phys. Rev. D **80**, 124051 (2009).
[9] B. J. Kelly, W. Tichy, Y. Zlochower, M. Campanelli, and B. Whiting, Classical Quantum Gravity **27**, 114005 (2010).
[10] F. Zhang and B. Szilágyi, Phys. Rev. D **88**, 084033 (2013).
[11] K. Slinker, C. R. Evans, and M. Hannam, Phys. Rev. D **98**, 044014 (2018).
[12] I. Ruchlin, Ph.D. thesis, Rochester Institute of Technology, 2015.
[13] U. Sperhake, V. Cardoso, C. D. Ott, E. Schnetter, and H. Witek, Phys. Rev. D **84**, 084038 (2011).
[14] K. Jani, J. Healy, J. A. Clark, L. London, P. Laguna, and D. Shoemaker, Classical Quantum Gravity **33**, 204001 (2016).
[15] L. Lindblom, B. J. Owen, and D. A. Brown, Phys. Rev. D **78**, 124020 (2008).